





Article

Rill and Interrill Soil Loss Estimations Using the USLE-MB Equation at the Sparacia Experimental Site (South Italy)

Vincenzo Pampalone ^{1,*} , Alessio Nicosia ¹ , Vincenzo Palmeri ¹ , Maria Angela Serio ¹ and Vito Ferro ^{1,2} 

¹ Department of Agricultural, Food and Forest Sciences, University of Palermo, Viale delle Scienze, Building 4, 90128 Palermo, Italy; alessio.nicosia@unipa.it (A.N.); vincenzo.palmeri02@unipa.it (V.P.); mariaangela.serio@unipa.it (M.A.S.); vito.ferro@unipa.it (V.F.)

² National Biodiversity Future Center (NBFC), 90133 Palermo, Italy

* Correspondence: vincenzo.pampalone@unipa.it

Abstract: A reliable prediction of event soil loss at the plot scale can be obtained by Universal Soil Loss Equation (USLE)-type models. For the Sparacia site (South Italy), the USLE-MB model was recently developed, in which the effect of the erosive agent is modeled using the rainfall erosivity index of the USLE by a power $b_1 > 1$ of the runoff coefficient Q_R . In this investigation, the model is parameterized separately using plot data collected for rill and interrill events that occurred in the Sparacia experimental area. The values $b_1 = 1.406$ and $b_1 = 1.012$ were obtained for the interrill and rill databases, respectively, which revealed a different effect of the runoff coefficient on soil loss due to the two erosive processes. Different relationships expressive of topographic factors were also deduced. The USLE-MB estimation performance significantly improved when operating the distinction between the two databases compared with the model parameterized on the complete database. The model was particularly reliable in estimating the highest event soil loss values, which were associated with the occurrence of rills. Finally, the proposed parameterization procedure lends itself to being tested in the framework of empirical soil loss modeling.

Keywords: water soil erosion; plot monitoring; soil erosion prediction; rainfall–runoff erosivity; interrill; rill



Citation: Pampalone, V.; Nicosia, A.; Palmeri, V.; Serio, M.A.; Ferro, V. Rill and Interrill Soil Loss Estimations Using the USLE-MB Equation at the Sparacia Experimental Site (South Italy). *Water* **2023**, *15*, 2396. <https://doi.org/10.3390/w15132396>

Academic Editors: Ian Prosser and Renato Morbidelli

Received: 15 May 2023
Revised: 26 June 2023
Accepted: 27 June 2023
Published: 28 June 2023



Copyright: © 2023 by the authors. Licensee MDPI, Basel, Switzerland. This article is an open access article distributed under the terms and conditions of the Creative Commons Attribution (CC BY) license (<https://creativecommons.org/licenses/by/4.0/>).

1. Introduction

Soil is an essential natural resource for food production and ecosystem functioning since it is a fundamental part of earth system functions that support the delivery of primary ecosystem services [1]. Water soil erosion is a natural process in which rainfall detaches soil particles from the soil surface and overland flow acts as a transport agent downslope, resulting in interrill erosion. If flow concentrates into rill channels, it can detach soil particles from the rill wetted perimeter and transport these sediments and those delivered from the interrill areas. In this case, both rill and interrill erosion occur, and the former usually prevails over the latter [2]. Accelerated erosion, which usually involves arable lands, can have strong and adverse impacts on soil and the environment [3], reducing the depth of the soil, which is substantially a non-renewable resource, and its agricultural productivity and producing sediments that can degrade water bodies. For example, accelerated soil loss can determine relevant sediment yield, which, in turn, produces enhanced flooding, reservoir oversedimentation and a lowering of water quality due to water turbidity and discharged pollutants. This implies the need to develop soil conservation strategies and models that can help with this task, even with the aim of simulating climate change scenarios that can enhance the negative impacts of soil erosion in different areas of the world [4]. The FAO-led Global Soil Partnership reports a soil loss of 75 billion tons per year from arable lands worldwide, which corresponds to an estimated loss of USD 400 billion per year [1]. According to [5], an average increase of 10–15% in rainfall erosivity and a similar increase

in soil loss rates are estimated till 2050 in Europe. For the Mediterranean zone, high erosion rates are estimated for many areas in Italy, including Sicily [6].

To predict soil erosion, conceptual, empirical, process-oriented, or physically based models have been developed. To avoid their misuse, they should be applied at the spatial (plot, hillslope, or basin) and temporal (event or year) scales for which they were developed. Process-oriented models (e.g., the Water Erosion Prediction Project (WEPP) [7] and the European Soil Erosion Model (EUROSEM) [8]) typically require collecting spatially distributed and sometimes difficult-to-obtain input data, while the Universal Soil Loss Equation (USLE) empirical modeling needs a parsimonious parameterization. Conversely, the limitations of the USLE are mainly related to the large temporal scale (mean annual) and to neglecting soil deposition phenomena that can also occur at the plot scale for which it was designed [9,10]. Some limitations were overcome in the evolutionary process of the USLE scheme. For example, the second revision of the USLE (RUSLE2) [11] works on a daily temporal scale and considers the deposition of soil particles in addition to detachment and transport. The model's performance does not always increase with its complexity. Tiwari et al. [12] and Morgan and Nearing [13] proved it for the more complex WEPP model, the USLE, and the revised USLE (RUSLE) [14] using 1600 and 1700 plot years of natural plot data, respectively. According to [15], the USLE, the RUSLE, and the WEPP, or other process-oriented models, constitute a complementary model suite to be chosen to meet the specific user need.

The recent review by the authors of [16] highlighted that the USLE and the RUSLE are by far the most widely applied soil erosion prediction models worldwide, with the latter being the subject of growing interest [17]. Rainfall erosivity is a driving factor for the USLE, RUSLE, and RUSLE2 [18]. Its mean annual value is determined by using the values calculated for each event as the product of the rainfall kinetic energy per unit area, E , and the maximum rainfall intensity with a duration of 30 min, I_{30} . A specific application of the USLE approach for event-based modeling was the USLE-M [19,20], which also considers event runoff Q_R in the event erosivity factor, $Q_R EI_{30}$. In the context of USLE-M type modeling, using bare plot data collected in the Sparacia (South Italy) experimental area, the USLE-MM [21,22] and the USLE-MB [23] were developed. In the former model, the event rainfall–runoff erosivity factor is $Q_R EI_{30}$ raised to a power greater than 1, while, in the latter, it is given by $Q_R^{b_1} EI_{30}$ with $b_1 > 1$. The USLE-MB has the following expression:

$$A_e = Q_R^{b_1} EI_{30} K_{MB} L_{MB} S_{MB} C_{MB} P_{MB}, \quad (1)$$

in which A_e (Mg ha^{-1}) is the event soil loss per unit area; K_{MB} is the soil erodibility factor; L_{MB} and S_{MB} are the plot length and steepness factors, respectively; C_{MB} is the cover and management factor; and P_{MB} is the support practice factor. The model was parameterized [18] for the bare plots of the Sparacia area maintained in a fallow condition ($C_{MB} = 1$, $P_{MB} = 1$) and was positively tested with data from bare plots of the Masse experimental station (Central Italy) [24].

Equation (1) was calibrated on the whole dataset available until 2018 without distinguishing between events with and without rill formation since the USLE approach addresses both interrill and rill erosion. However, soil-erosion-controlling variables affect interrill and rill erosion differently, and this is actually accounted for by different components in the process-based erosion models [25]. From this consideration and taking into account that, for rill events at the Sparacia area, total erosion is mainly due to the rill component [26], the question of whether the USLE-MB estimation performance improves with two independent parameterizations regarding interrill and rill data is raised. To the best of our knowledge, there have been no attempts in the literature to test this hypothesis for USLE-based models; therefore, the present investigation could suggest procedural improvements in soil loss estimation by empirical modeling in different areas of interest. The aim of this investigation is to (i) calibrate the USLE-MB with the entire Sparacia dataset, which is larger than that available in 2018, to improve the robustness of the model and

(ii) to calibrate the model separately for rill and interrill events to evaluate the effectiveness of discriminating the two erosive forms for better event soil loss prediction.

2. Materials and Methods

2.1. Experimental Plots and Datasets

The experimental plots for monitoring event soil loss are installed in the Sparacia site (western Sicily, southern Italy) and are characterized by clay soil (62% clay, 33% silt, and 5% sand) and different sizes and steepness values, which are summarized in Table 1. Twenty-two Wischmeier plots (Figure 1), maintained in cultivated fallow, are equipped and arranged in different plot types, i.e., with a given combination of length λ and steepness s . Rainfall intensity is measured by two recording rain gauges installed close to the 14.9% and 22% sloped hillslopes.

During an erosive event, the suspension (plot runoff and sediments) is collected into the tanks arranged in series at the plot outlet. Runoff and soil loss measurements are carried out when a rainfall event or a series of temporally close events produce measurable sediment amounts.

The plot soil loss is measured as the product of the mean concentration and suspension volume. The latter is determined by the suspension level reading, given the geometric characteristics of the tanks. The mean concentration measurement procedure is described in detail by [27] and is not reported here for the sake of brevity.

During the monitoring period, plots were subjected to erosive events in which only interrill erosion or interrill and rill erosion occurred. The former took place much more frequently than the latter. Rills were always obliterated by tillage with a power cultivator after the field survey.

Table 1. Values of the b_1 exponent obtained from the regression of A_e/EI_{30} vs. Q_R on logarithmically transformed data for different plot types and databases (complete, C-Db–Interrill, I-Db–and Rill, and R-Db).

$\lambda \times w$ (m × m)	s (-)	Number of Plots	C-Db				I-Db				R-Db			
			b_1	R^2	p	n	b_1	R^2	p	n	b_1	R^2	p	n
22 × 2	0.09	2	1.173	0.53	0.0003	20	0.951 *	0.31	0.0169	18				
11 × 2 and 11 × 4	0.149	4	1.398	0.54	0.0000	119	1.294	0.48	0.0000	102	1.046	0.74	0.0000	17
22 × 2 and 22 × 8	0.149	8	1.541	0.63	0.0000	282	1.388	0.59	0.0000	240	0.966	0.51	0.0000	42
33 × 8	0.149	2	1.650	0.72	0.0000	99	1.565	0.70	0.0000	84	1.000	0.47	0.0045	15
44 × 8	0.149	2	1.751	0.65	0.0000	63	1.665	0.60	0.0000	57	0.241 *	0.05	0.672	6
22 × 6	0.22	2	1.208	0.43	0.0000	74	1.214	0.51	0.0000	53	0.832	0.36	0.0039	21
22 × 6	0.26	2	1.254	0.32	0.0000	63	1.310	0.35	0.0000	51	1.214	0.52	0.0079	12

Notes: λ = Plot length, w = plot width, s = plot steepness, R^2 = coefficient of determination of the regression, n = sample size, and * = not statistically significant at a significance level of 0.01.

For each erosive event, the total rainfall depth, P_e (mm), and the event rainfall erosivity index, EI_{30} ($\text{MJ mm h}^{-1} \text{ha}^{-1}$) [28], were determined. Simultaneous measurements of event runoff and soil loss from individual plots were selected from the Sparacia database since USLE-MB also requires the hydrological information to be applied. In other words, plot measurements not including runoff were not considered. For each plot and event, the total runoff per unit area, V_e (mm), the runoff coefficient, $Q_R = V_e/P_e$, and the soil loss per unit area, A_e (Mg ha^{-1}), were determined. The complete dataset (C-Db) used here consists of $N = 720$ measurements and was also split into two different datasets, i.e., one for the measurements derived from only interrill erosion (I-Db, $N = 605$) and one for those derived from both interrill and rill erosion (R-Db, $N = 115$) (Table 2). The rainfall depth for the I-Db was, on average, higher than the corresponding value in the R-Db, while

the rainfall erosivity factor was sharply lower. This signals that, as expected, rills mainly formed due to intense rainfall events. The values of runoff coefficient and soil loss for R-Db were, on average, higher than for I-Db and had lower variability. Therefore, although the experimental ranges of P_e , EI_{30} , Q_R , and A_e for the I-Db and R-Db were partially overlapped, both the main rainfall characteristics and the plot hydrological and erosive response varied between the two databases.

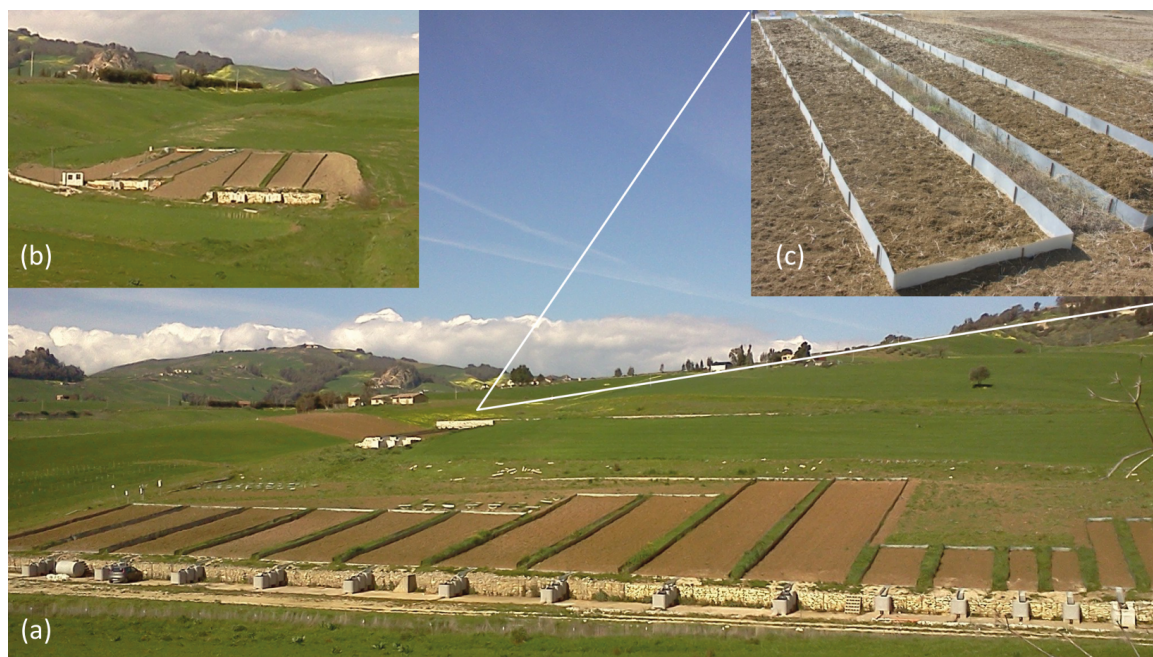


Figure 1. View of the plots with slope gradient s equal to (a) 0.149, (b) 0.22 and 0.26, and (c) 0.09 at Sparacia experimental area.

Table 2. Summary statistics of the rainfall depth P_e (mm); rainfall erosivity factor EI_{30} ($\text{MJ mm ha}^{-1}\text{h}^{-1}$); runoff coefficient Q_R (-); Q_REI_{30} ($\text{MJ mm ha}^{-1}\text{h}^{-1}$); and soil loss A_e (Mg ha^{-1}) values for the complete database (C-Db), interrill database (I-Db), and rill database (R-Db).

Database	Statistic	P_e	EI_{30}	Q_R	Q_REI_{30}	A_e
C-Db	min	11.8	8.05	0.0011	0.058	0.0012
	max	145.8	988.8	0.81	508.2	272.9
	mean	46.8	166.5	0.13	21.6	9.4
	median	41.6	104.9	0.09	11.3	1.5
	CV	0.60	0.93	0.93	1.7	2.3
I-Db	min	11.8	8.05	0.0011	0.058	0.0012
	max	145.8	469.8	0.74	71.0	92.5
	mean	48.6	134.3	0.11	12.6	4.0
	median	42	103.9	0.07	9.2	0.7
	CV	0.60	0.78	1.00	1.0	2.0
R-Db	min	14.8	57.9	0.03	2.6	1.15
	max	97.8	988.8	0.81	508.2	272.9
	mean	37.3	336.0	0.20	69.0	38.0
	median	33	265.3	0.18	41.3	27.5
	CV	0.46	0.73	0.57	1.0	1.1

2.2. Model Parameterization

To determine the exponent b_1 of the runoff coefficient, the regression of A_e/EI_{30} versus Q_R was performed using the complete, the interrill, and the rill databases. The statistical analysis allowed for the individuation of differences between the three values of the b_1

coefficient, which were considered in the subsequent model parameterization. Specifically, a single parameterization was carried out for each of the three databases from the bare plots, for which $C_{MB} = 1$ and $P_{MB} = 1$. The $K_{MB} L_{MB} S_{MB}$ experimental value for a given plot type was calculated by the following relationship [23]:

$$K_{MB} L_{MB} S_{MB} = \frac{\sum_{i=1}^N A_{e,i}}{\sum_{i=1}^N (EI_{30} Q_R^{b1})_i} \quad (2)$$

When $\lambda = 22$ m ($L_{MB} = 1$ by definition), the equation reduces to

$$K_{MB} S_{MB} = \frac{\sum_{i=1}^N A_{e,i}}{\sum_{i=1}^N (EI_{30} Q_R^{b1})_i} \quad (3)$$

An interpolating s - $K_{MB} S_{MB}$ relationship passing from the origin of the axes was determined for the 22 m long plots ($s = 14.9, 22$, and 26%). The extrapolation of this relationship to $s = 9\%$ allowed us to estimate K_{MB} as S_{MB} was set equal to 1 for this plot steepness. Consequently, the site-specific S_{MB} relationship was also determined. The $K_{MB} L_{MB} S_{MB}$ values calculated using Equation (2) for $\lambda = 11, 33$, and 44 m were divided by the estimated $K_{MB} S_{MB}$ value for $s = 14.9\%$ to determine the experimental L_{MB} for each of the three plot lengths, while L_{MB} was set equal to 1 for $\lambda = 22$ m. Finally, the relationship of L_{MB} against λ was deduced.

2.3. Performance of the USLE-MB Model

The evaluation of the USLE-MB parameterized on the three different datasets was conducted by a visual inspection of the comparison between measured and estimated soil losses and three quantitative statistics, i.e., the Nash–Sutcliffe model efficiency index, $NSEI$; the root-mean-square error, $RMSE$; and the $BIAS$. The $NSEI$ expresses the extent of the residual variance relative to the measurement variance and indicates the closeness among the pairs of measured and estimated soil loss and the perfect agreement line. The $NSEI$ is calculated as

$$NSEI = 1 - \frac{\sum_{i=1}^N (A_{e,measured} - A_{e,calculated})_i^2}{\sum_{i=1}^N (A_{e,measured} - A_{e,mean})_i^2} \quad (4)$$

where $A_{e,measured}$ and $A_{e,calculated}$ are the measured and calculated soil loss, respectively, and $A_{e,mean}$ is the mean of the soil loss measurements. The null and positive values of this index indicate the improved estimation performances of the model from the situation in which the predictions are as accurate as the mean measured value ($NSEI = 0$) to that in which the calculated values coincide with the measured values ($NSEI = 1$). The predictions are worse than the sample mean when $NSEI$ is negative. The $RMSE$ has the following expression:

$$RMSE = \sqrt{\frac{\sum_{i=1}^N (A_{e,measured} - A_{e,calculated})_i^2}{N}} \quad (5)$$

It quantifies the deviation between predictions and measurements in the units of the measurement variable. The model performance improves with decreasing values of the $RMSE$. Finally, the $BIAS$ is calculated by the following relationship:

$$BIAS = \frac{\sum_{i=1}^N (A_{e,measured} - A_{e,calculated})_i}{N} \quad (6)$$

Positive values are indicative of model underestimations, negative values are indicative of overestimations, and $BIAS = 0$ if the model is unbiased.

For the model version with the best performance, the quantitative statistics were also calculated for three severity levels of soil loss, discriminating by $A_e = 1$ Mg ha⁻¹ and 10 Mg ha⁻¹. Specifically, for both the interrill and rill databases, three classes of soil loss,

i.e., lower than 1 Mg ha^{-1} , ranging from 1 to 10 Mg ha^{-1} , and higher than 10 Mg ha^{-1} , were distinguished, and the values of the *BIAS* and $RMSE/\mu(A_e)$, where $\mu(A_e)$ is the mean soil loss, were calculated for each of them.

3. Results

3.1. Rainfall–Runoff Erosivity Factor

The plot of A_e/EI_{30} against Q_R shows, as an example for $\lambda = 22$ and 33 m and $s = 14.9\%$ (Figure 2), that the experimental pairs of the rill database fall in the upper right part of the scatterplots. Therefore, both the soil loss per unit of EI_{30} and the runoff coefficient associated with the rill measurements are higher than those of the interrill database. In addition, the difference in the interpolating power relationships induced the regression of A_e/EI_{30} vs. Q_R for each plot type by considering separately the interrill, rill, and complete, i.e., not distinguishing between rill and interrill measurements, datasets for comparative purposes.

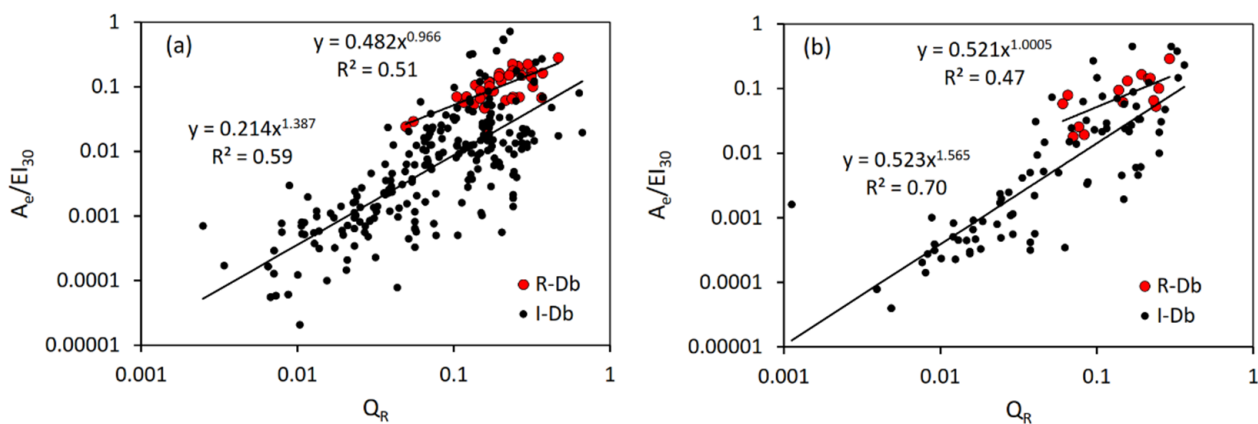


Figure 2. Comparison between the experimental pairs (Q_R and A_e/EI_{30}) and the regression lines for the rill and interrill databases for the plots with a slope gradient of $s = 0.149$ and lengths of (a) $\lambda = 22 \text{ m}$ and (b) $\lambda = 33 \text{ m}$.

The regression of A_e/EI_{30} vs. Q_R on logarithmically transformed data was statistically significant ($p < 0.01$) for all plot types but two ($\lambda = 22 \text{ m}$ and $s = 0.09$ for the I-Db; $\lambda = 44 \text{ m}$ and $s = 14.9\%$ for the R-Db) (Table 1). For the statistically significant regressions, the determination coefficient, R^2 , varied from 0.35 to 0.70 (I-Db), 0.36 to 0.74 (R-Db), and 0.32 to 0.72 (C-Db). Table 1, which lists the b_1 values for each plot type and dataset, highlights that they range from 1.21 to 1.67 for the I-Db and from 0.83 to 1.21 for the R-Db. The b_1 values statistically differ between the I-Db and R-Db databases as those related to a given database tend to (five out of seven cases) fall out of the confidence interval at the probability level of 95% in relation to the other database (Figure 3a,b). For the complete dataset, b_1 varies between 1.17 and 1.75 (Figure 3c,d). Figure 3 shows that b_1 can be considered independent of plot length and steepness except for the two cases in which an increasing relationship of b_1 versus λ was detected (I-Db and C-Db). However, following [23], the slope and length effects on soil loss were attributed exclusively to the topographic factors, and the mean values $b_1 = 1.406$ and $b_1 = 1.012$ have been applied hereinafter for the I-Db and R-Db, respectively. These values are representative of the two databases as they fall within the confidence intervals for b_1 for all investigated plots (Figure 3a,b). To meet this criterion, the mean value weighted with the sample size of each plot type ($b_1 = 1.481$) was applied for the C-Db (Figure 3c,d).

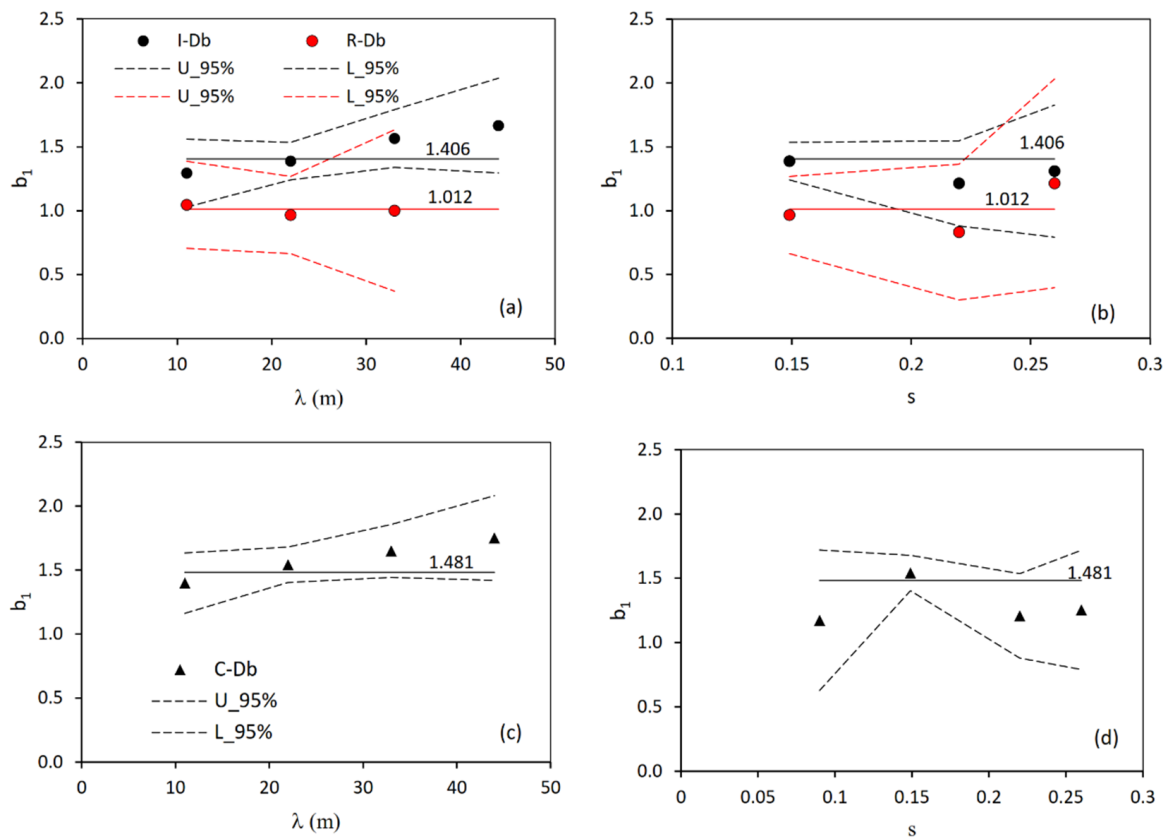


Figure 3. Relationship between the exponent b_1 and (a) plot length, λ , for a slope steepness, s , of 14.9% for the interrill and rill databases; (b) s for the interrill and rill databases; (c) λ for the complete database; and (d) s for the complete database. U = Upper limit of the 95% occurrence interval. L = Lower limit of the 95% occurrence interval.

3.2. Determination of the Soil Erodibility Factor and the Topographic Factors of the USLE-MB

The K_{MB} S_{MB} values calculated by Equation (3), with the specific b_1 value for each dataset, were described by the following relationship [22,23,29]:

$$K_{MB}S_{MB} = a_0[\exp(bs) - 1] \tag{7}$$

where the a_0 and b coefficients are equal to 0.45 and 4.0 for the C-Db, 0.27 and 6.64 for the I-Db, and 63.48 and 0.06 for the R-Db. For $s = 0.09$ ($S_{MB} = 1$), Equation (7) gives $K_{MB} = 0.412$ (C-Db), 0.222 (I-Db), and 0.334 (R-Db), which yield the following expressions of the slope steepness factor (Figure 4):

$$S_{MB} = 2.31[\exp(4.0s) - 1](C - Db) \tag{8}$$

$$S_{MB} = 1.22[\exp(6.64s) - 1](I - Db) \tag{9}$$

$$S_{MB} = 190.27[\exp(0.06s) - 1](R - Db) \tag{10}$$

The experimental values of the L_{MB} factor were then obtained by combining Equations (2) and (7):

$$L_{MB} = \frac{\sum_{i=1}^N A_{e,i}}{\sum_{i=1}^N (Q_R^{b_1} EI_{30})_i} \frac{1}{a_0[\exp(bs) - 1]} \tag{11}$$

With the assumption of $L_{MB} = 1$ for $\lambda = 22$ m, this allowed determining the plot length factor expressions (Figure 5):

$$L_{MB} = \left(\frac{\lambda}{22}\right)^{0.91} (C - Db) \tag{12}$$

$$L_{MB} = \left(\frac{\lambda}{22}\right)^{0.58} \text{ for } \lambda \leq 22 \text{ m(I - Db) and (R - Db)} \tag{13}$$

$$L_{MB} = \left(\frac{\lambda}{22}\right)^\alpha \text{ for } 22 \text{ m} \leq \lambda \leq 44 \text{ m(I - Db) and (R - Db)} \tag{14}$$

where $\alpha = 1.55$ for the I-Db, and $\alpha = 0$ for the R-Db. Finally, the USLE-MB for the Sparacia site is expressed as

$$A_e = \left(Q_R^{1.481} EI_{30}\right) 0.412 \left(\frac{\lambda}{22}\right)^{0.91} 2.31[\exp(4.0s) - 1](C - Db) \tag{15}$$

$$A_e = \left(Q_R^{1.406} EI_{30}\right) 0.222 \left(\frac{\lambda}{22}\right)^{0.58} 1.22[\exp(6.64s) - 1] \text{ for } \lambda \leq 22 \text{ m(I - Db)} \tag{16a}$$

$$A_e = \left(Q_R^{1.406} EI_{30}\right) 0.222 \left(\frac{\lambda}{22}\right)^{1.55} 1.22[\exp(6.64s) - 1] \text{ for } 22 \text{ m} \leq \lambda \leq 44 \text{ m(I - Db)} \tag{16b}$$

$$A_e = \left(Q_R^{1.012} EI_{30}\right) 0.334 \left(\frac{\lambda}{22}\right)^{0.58} 190.27[\exp(0.06s) - 1] \text{ for } \lambda \leq 22 \text{ m(R - Db)} \tag{17a}$$

$$A_e = \left(Q_R^{1.012} EI_{30}\right) 0.334 190.27[\exp(0.06s) - 1] \text{ for } 22 \text{ m} \leq \lambda \leq 44 \text{ m(R - Db)} \tag{17b}$$

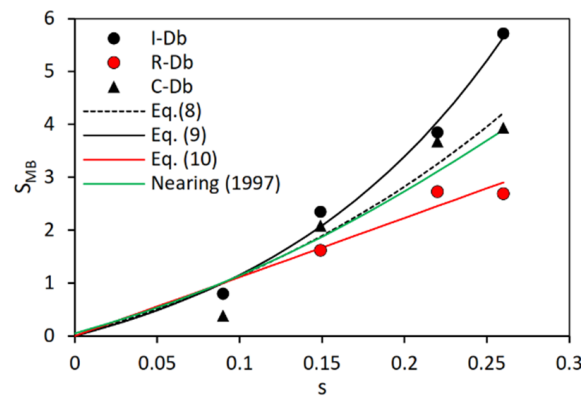


Figure 4. Plot of the steepness factor, S_{MB} , against plot steepness, s , for the interrill, rill, and complete databases; Equations (8)–(10); and the expression provided by the authors of [30] for the 22 m long plots.

Equations (15)–(17) point out the influence of the parameterization database on the soil loss prediction model.

For the complete dataset, b_1 was also determined by the linear regression of the log-transformed (Q_R and $A_e / (L_{MB} S_{MB} EI_{30})$) experimental pairs (Figure 6) using the expressions by [14,30] for L_{MB} and S_{MB} , respectively. The latter are reported in the square brackets in the following USLE-MB equation:

$$A_e = \left(Q_R^{1.56} EI_{30}\right) 0.505 \left[\left(\frac{\lambda}{22.13}\right)^{\frac{\sin\beta}{0.0896(3\sin^{0.8}\beta + 0.56)} + \frac{1}{0.0896(3\sin^{0.8}\beta + 0.56)}} \right] \left[-1.5 + \frac{17}{1 + \exp(2.3 - 6.1\sin\beta)} \right] \tag{18}$$

where $\beta(^{\circ})$ is the slope angle. The exponent $b_1 = 1.56$ was estimated by the applied regression, and the soil erodibility $K_{MB} = 0.505$ was calculated using Equation (2) with $b_1 = 1.56$ [24].

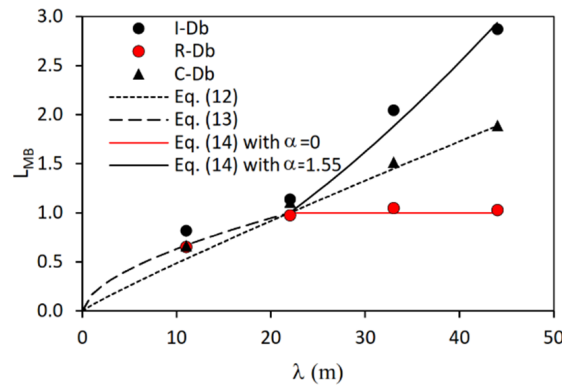


Figure 5. Plot of the plot length factor, L_{MB} , against plot length, λ , for the interrill, rill, and complete databases and Equations (12)–(14).

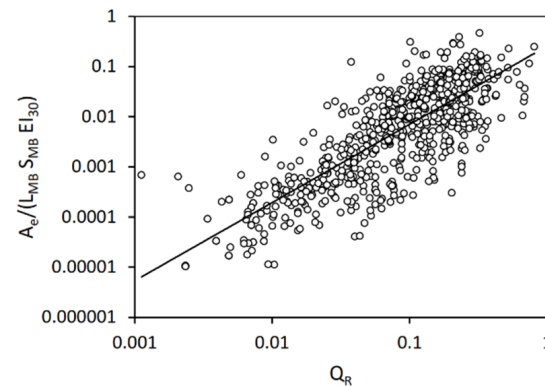


Figure 6. Plot of the experimental pairs (Q_R and $A_e / (L_{MB} S_{MB} E I_{30})$) of the complete dataset, where L_{MB} and S_{MB} are given by the expressions provided in [14,30], respectively, and the regression curve yielding $b_1 = 1.56$.

3.3. Comparing USLE-MB Equations

A comparison between the estimation performances of Equations (15) and (18) and the performances of Equations (16) and (17) combined was performed. Equations (16) and (17) were alternatively applied to estimate soil loss according to the detected erosive component (interrill or rill) for the 720 measurements. Even though the quantitative statistics reported in Table 1 highlight that the coupled Equations (16) and (17) perform only slightly better than Equations (15) and (18), Figure 7 shows a significant improvement in soil loss prediction by Equations (16) and (17), especially for highly erosive events characterized by rill occurrence. The scatterplots of measured vs. calculated soil loss values by Equations (15) and (18) do not show relevant differences (Figure 7a,c), even though Table 1 signals a better estimation performance for Equation (18).

For the more reliable model (Equations (16) and (17)), a specific error analysis was carried out, and the quantitative statistics for three severity levels of soil loss and both the I-Db and R-Db are listed in Table 2. For each database, the $RMSE / \mu(A_e)$ decreases with increasing severity levels and, for a given severity level, in the passage from the I-Db to the R-Db. The $BIAS$ values for the two datasets indicate a low and comparable soil loss overestimate for the intermediate severity level and a sharp underestimate of the highest soil loss values ($A_e > 10 \text{ Mg ha}^{-1}$) for the I-Db. For the high severity level and the R-Db, instead, the $BIAS$ is close to 0.

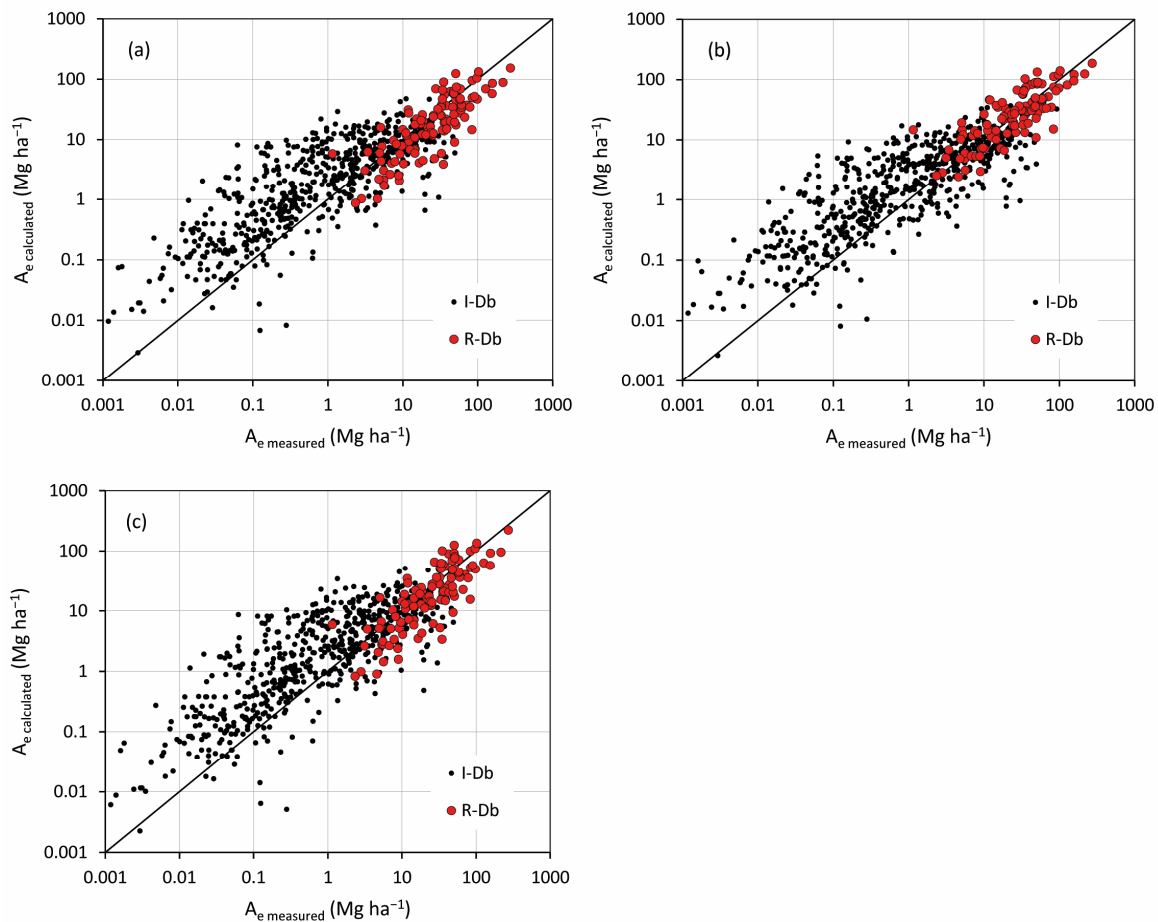


Figure 7. Comparison between measured and predicted soil loss values for (a) Equation (15), (b) Equations (16) and (17), and (c) Equation (18).

4. Discussion

4.1. Rainfall–Runoff Erosivity Factor and Soil Erodibility Factor

Previous investigations [23,24] suggested that the rainfall–runoff erosivity factor can be considered equal to $EI_{30} Q_R^{1.2}$ and that the event soil erodibility factor, $Q_R^{b_1-1.2} K_{MB}$, consists of a stationary component, K_{MB} , and a dynamic hydrological component, $Q_R^{b_1-1.2}$. This result originated from the parameterization of the USLE-MB with 570 ($b_1 = 1.46$, [23]) and 641 ($b_1 = 1.52$, [24]) plot measurements without a distinction between rill and interrill erosion data. The runoff erosivity factor was imposed to be $Q_R^{1.2}$. It was physically related to flow transport capacity since, according to the scheme of the process-oriented WEPP model and for uniform shallow flow, the latter is proportional to the 1.2 power of the unit flow discharge [31], and Q_R is representative of the unit discharge. The dynamic hydrological component of the soil erodibility, $Q_R^{b_1-1.2}$, corrects the stationary one, K_{MB} , accounting for the effect of the inter-event variability, which was also detected in the USLE context [32–35].

This formulation was confirmed here for the I-Db and the C-Db but not for the R-Db. For the I-Db, the flow discharge is routed as shallow flow, and the transport capacity is proportional to the 1.2 power of the unit discharge. Instead, for channelized flows (R-Db) with the same discharge, the flow features a higher mean velocity and a greater transport capacity. Therefore, the transport capacity can be simply proportional to the unit discharge (Q_R), $EI_{30} Q_R$ expresses the rainfall–runoff erosivity factor, and the soil erodibility factor is stationary. The inter-event variability of the soil erodibility does not occur for the R-Db events, probably because there are negligible temporal heterogeneities in the controlling factors, such as soil aggregate stability or shear strength [36–39], once rill channels have

been formed due to such highly erosive events. Finally, the dominance of the interrill measurements ($N = 605$) with respect to the rill ones ($N = 115$) affects the result obtained with the C-Db. In other words, the distinction between the two datasets allowed for highlighting what is hidden in the current C-Db and in the previous investigations [23,24]. The dominance of the interrill measurements is also the reason why b_1 was found to increase with plot length for the C-Db as well as for the I-Db, even though b_1 was practically independent of λ for the R-Db.

For the R-Db, the USLE-MB reduces to USLE-M ($b_1 = 1$). Considering that soil loss is equal to runoff by sediment concentration, the applicability of the USLE-M implies that the sediment concentration is proportional to EI_{30}/P_e [19]. When the USLE-MB applies, the sediment concentration is proportional to EI_{30}/P_e and the power b_1-1 of Q_R . For given rainfall characteristics, the runoff volume V_e does not influence sediment concentration in the former case, whereas it does in the latter.

4.2. Topographic Factors

The slope length factor increased for I-Db and R-Db according to two different relationships that coincide and overlap with the expression proposed by [30] for s values less than 9% alone; however, these are out of the investigated range. For $s > 9\%$, this expression from the literature is intermediate between the two relationships and practically coincides with that (Equation (8)) calibrated on the C-Db. This last result suggests that the equation by [30] is applicable for the USLE-MB calibrated at the Sparacia station on the C-Db, confirming the result by [23], while it is not applicable for the other two cases.

For both the rill and interrill databases, the plot length factor was assumed to increase with plot lengths up to $\lambda = 22$ m according to a relationship (Equation (13)), which is practically consistent with the RUSLE model [14]. Above this plot length value, for the I-Db, the plot length factor continues to increase with λ but according to a different power relationship (Equation (14) with $\alpha = 1.55$), while it is constant for the R-Db (Equation (14) with $\alpha = 0$).

Even though $L_{MB}S_{MB}$ for the I-Db is greater than or equal to that corresponding to the R-Db (Figures 4 and 5), the estimated values by Equation (17) (R-Db) are higher than those predicted by Equation (16) (I-Db) as the rainfall-runoff erosivity factor $Q_R^{b_1}EI_{30}$ in the former case is generally higher than in the latter.

The relationships that express the plot length and slope effects on soil loss are not sufficient to determine the pattern of estimated soil loss per unit area by Equations (15)–(17) with λ and s . This pattern also depends on the relationship between the plot runoff coefficient and topographic characteristics. The analysis developed by [40] using plot data from Sparacia station highlighted that a lack of statistically detectable plot length effects on event runoff and soil loss per unit area was the prevailing result, and, in the presence of scale effects, runoff decreased and soil loss per unit area generally decreased with plot length. Figure 8 confirms, for a larger overall database than that presented in [40] and the interrill and rill sub-datasets, the reduction in the runoff coefficient with increasing λ . For the plot data from the Sparacia area, Bagarello et al. [41] demonstrated that Q_R did not vary appreciably with slope steepness s , while A_e increased with s . In light of the deduced expressions for the topographic factors and the relations between the plot topographic characteristics and the runoff coefficient, Equations (15)–(17) allow a prediction of soil loss per unit area that does not increase with plot length but increases with plot steepness, which is consistent with the experimentally observed phenomenon. A decreased soil loss per unit area for longer plots is especially evident for the R-Db from Figure 5 ($L_{MB} = \text{constant}$ for $\lambda \geq 22$ m) and Figure 8 (the mean decreasing rate of Q_R with λ is higher for the R-Db than the I-Db). Previous results regarding the plot length effects on the rill and interrill rates and the corresponding total soil loss, A_e , detected for four erosion events [41–43] included in the R-Db by definition, suggested that this result is due to increasing rill erosion rates and decreasing interrill erosion rates or increasing deposition phenomena in the interrill areas.

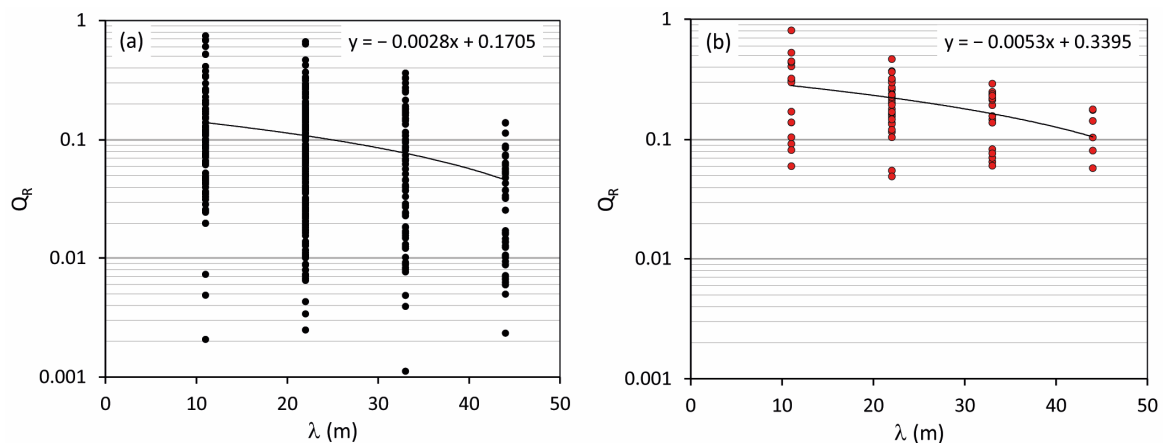


Figure 8. Relationship between the runoff coefficient Q_R and the plot length λ for the (a) interrill and (b) rill databases.

4.3. Comparing USLE-MB Equations

The comparison among Equations (15)–(18) highlighted that there is no advantage in the parameterization of the USLE-MB model on the C-Db compared with the simple use of the literature expressions to estimate the topographic factors and a single regression analysis to determine the runoff exponent b_1 . Instead, the estimation performance significantly improves if the model is parameterized separately for the I-Db and R-Db.

The error indexes listed in Table 2 point out that the USLE-MB expressed by Equation (17) is particularly able to predict the highest soil losses associated with the presence of rills. This result is also particularly encouraging as soil loss values greater than 10 Mg ha^{-1} are numerically predominant in the R-Db (91 out of 115 soil loss measurements).

Currently, the USLE-MB cannot be proposed for general use since values of b_1 have been deduced for only Masse (Central Italy) [24] and Sparacia complete datasets till now. Even though the b_1 exponent varied between the Sparacia and Masse sites, the related analysis [24] demonstrated that the use of a common exponent was statistically supported. Nothing can still be said about the general validity of raising the Q_R term to an exponent greater than one only for the interrill data in contrast with an exponent of about one for the rill data. Therefore, there is a need to experimentally test this result both at Masse and other sites to establish if an independent parameterization for rill and interrill data is advisable to be performed in general.

The use of the USLE-MB equation for predictive purposes requires simple and accurate methods to estimate runoff at the event and plot scales, and, to gain better soil loss predictions, the ability to distinguish between events with only interrill erosion and events with both rill and interrill erosion is required. Some positive results were recently achieved [44–46] concerning runoff prediction with simple approaches, including, for example, the Soil Conservation Service curve number. As for the other issue, a recent investigation [47], based on the Sparacia and Masse datasets, allowed for determining the threshold values of some rainfall variables able to distinguish between (i) erosive and no-erosive rains and (ii) rainfall events with only interrill erosion and with rill development. For the Sparacia dataset, the best variables for identifying rill events were mean rainfall intensity, i.e., the ratio between the event rainfall amount and the event total duration, and the so-called mean wet rainfall intensity, i.e., the ratio between the event rainfall amount and the cumulative duration of only the continuous rain showers within the event. Specifically, the criteria of a mean rainfall intensity higher than or equal to 8.9 mm h^{-1} and a mean wet rainfall intensity higher than or equal to 15 mm h^{-1} correctly identified more than 53% of events with rill development. Developing this type of analysis in other experimental sites could enhance the practical interest for the USLE-MB.

5. Conclusions

Soil erosion prediction models using the USLE approach are widely applied because they combine a simple mathematical structure and parsimonious parameterization with a similar uncertainty to that of more complex process-oriented models. The evolution of USLE-type modeling incorporates a consideration of runoff into event-based prediction, as in the case of the USLE-MB.

In this paper, the exponent b_1 of the runoff coefficient was dependent on the parameterization database, resulting in $b_1 = 1.406$ and $b_1 = 1.012$ for the interrill and rill data, respectively. This result depends on the fact that, for a given discharge, rill flows have a higher mean velocity and transport capacity than interrill flows. Site-specific relationships for the topographic factors were deduced for rill and interrill data. The parameterized models allow a prediction of soil loss per unit area, which does not necessarily increase with plot length but increases with plot steepness, agreeing with the observed erosion phenomenon at the Sparacia experimental area.

The USLE-MB reliability significantly improved after adopting the independent parameterization for rill and interrill data. Moreover, the model was particularly accurate in the prediction of the highest soil loss values, which are the most relevant from a practical point of view as they can control the total soil loss of an area.

The soil loss prediction by the USLE-MB needs simple and accurate methods to estimate plot runoff at the event scale and hopefully identify the erosion pattern that will occur. Considering the available literature, these appear to be practically affordable tasks.

Author Contributions: Conceptualization, V.P. (Vincenzo Pampalone), A.N., V.P. (Vincenzo Palmeri), M.A.S. and V.F.; methodology, V.P. (Vincenzo Pampalone), A.N., V.P. (Vincenzo Palmeri), M.A.S. and V.F.; formal analysis, V.P. (Vincenzo Pampalone), A.N., V.P. (Vincenzo Palmeri), M.A.S. and V.F.; investigation, V.P. (Vincenzo Pampalone), A.N., V.P. (Vincenzo Palmeri), M.A.S. and V.F.; writing—original draft preparation, V.P. (Vincenzo Pampalone), A.N., V.P. (Vincenzo Palmeri), M.A.S. and V.F.; writing—review and editing, V.P. (Vincenzo Pampalone), A.N., V.P. (Vincenzo Palmeri), M.A.S. and V.F. All authors have read and agreed to the published version of the manuscript.

Funding: This study was carried out within the RETURN Extended Partnership and received funding from the European Union Next-GenerationEU (National Recovery and Resilience Plan—NRRP, Mission 4, Component 2, Investment 1.3—D.D. 1243 2/8/2022, PE0000005).

Data Availability Statement: The data that support the findings of this study are available from the corresponding author upon reasonable request. The availability of data for future research developments needs the involvement of the research group of the University of Palermo.

Conflicts of Interest: The authors declare no conflict of interest. The funders had no role in the design of the study; in the collection, analyses, or interpretation of data; in the writing of the manuscript; or in the decision to publish the results.

References

1. Borrelli, P.; Robinson, D.A.; Fleischer, L.R.; Lugato, E.; Ballabio, C.; Alewell, C.; Meusburger, K.; Modugno, S.; Schütt, B.; Ferro, V.; et al. An assessment of the global impact of 21st century land use change on soil erosion. *Nat. Commun.* **2017**, *8*, 2013. [[CrossRef](#)] [[PubMed](#)]
2. Di Stefano, C.; Ferro, V.; Pampalone, V. Modeling Rill Erosion at the Sparacia Experimental Area. *J. Hydrol. Eng.* **2015**, *20*, C5014001. [[CrossRef](#)]
3. Di Stefano, C.; Ferro, V. Establishing soil loss tolerance: An overview. *J. Agric. Eng.* **2016**, *XLVII*, 127–133. [[CrossRef](#)]
4. Borrelli, P.; Robinson, D.A.; Panagos, P.; Lugato, E.; Yang, J.E.; Alewell, C.; Wuepper, D.; Montanarella, L.; Ballabio, C. Land use and climate change impacts on global soil erosion by water (2015–2070). *Proc. Natl. Acad. Sci. USA* **2020**, *117*, 21994–22001. [[CrossRef](#)] [[PubMed](#)]
5. Panagos, P.; Borrelli, P.; Poesen, J.; Ballabio, C.; Lugato, E.; Meusburger, K.; Montanarella, L.; Alewell, C. The new assessment of soil loss by water erosion in Europe. *Environ. Sci. Policy* **2015**, *54*, 438–447. [[CrossRef](#)]
6. Cerdan, O.; Govers, G.; Le Bissonnais, Y.; Van Oost, K.; Poesen, J.; Saby, N.; Gobin, A.; Vacca, A.; Quinton, J.; Auerswald, K.; et al. Rates and spatial variations of soil erosion in Europe: A study based on erosion plot data. *Geomorphology* **2010**, *122*, 167–177. [[CrossRef](#)]

7. Nearing, M.A.; Foster, G.R.; Lane, L.J.; Finkner, S.C. A Process-Based Soil Erosion Model for USDA-Water Erosion Prediction Project Technology. *Trans. ASAE* **1989**, *32*, 1587–1593. [[CrossRef](#)]
8. Morgan, R.P.C.; Quinton, J.N.; Smith, R.E.; Govers, G.; Poesen, J.W.A.; Auerswald, K.; Chisci, G.; Torri, D.; Styczen, M.E. The European soil erosion model (EUROSEM): A process-based approach for predicting soil loss from fields and small catchments. *Earth Surf. Process. Landf.* **1998**, *23*, 527–544. [[CrossRef](#)]
9. Di Stefano, C.; Ferro, V.; Pampalone, V.; Sanzone, F. Field investigation of rill and ephemeral gully erosion in the Sparacia experimental area, South Italy. *Catena* **2013**, *101*, 226–234. [[CrossRef](#)]
10. Rejman, J.; Brodowski, R. Rill characteristics and sediment transport as a function of slope length during a storm event on loess soil. *Earth Surf. Process. Landf.* **2005**, *30*, 231–239. [[CrossRef](#)]
11. USDA. *Revised Universal Soil Loss Equation Version 2 (RUSLE2)*; Science documentation; USDA-Agricultural Research Service: Washington, DC, USA, 2008.
12. Tiwari, A.K.; Risse, L.M.; Nearing, M.A. Evaluation of WEPP and its comparison with usle and rusle. *Trans. ASAE* **2000**, *43*, 1129–1135. [[CrossRef](#)]
13. Morgan, R.P.C.; Nearing, M.A. *Handbook of Erosion Modelling*; John Wiley and Sons: Hoboken, NJ, USA, 2011; pp. 1–401.
14. Renard, K.G.; Foster, G.R.; Weesies, G.A.; McCool, D.K.; Yoder, D.C. Predicting Soil Erosion by Water: A Guide to Conservation Planning with the Revised Universal Soil Loss Equation (RUSLE). In *USDA Agriculture Handbook, 703*; USDA: Washington, DC, USA, 1997.
15. Nearing, M.A. 22-Soil erosion and conservation. In *Environmental Modelling: Finding Simplicity in Complexity*, 2nd ed.; Wainwright, J., Mulligan, M., Eds.; John Wiley & Sons, Ltd.: Hoboken, NJ, USA, 2013; pp. 365–378.
16. Alewell, C.; Borrelli, P.; Meusburger, K.; Panagos, P. Using the USLE: Chances, challenges and limitations of soil erosion modelling. *Int. Soil Water Conserv. Res.* **2019**, *7*, 203–225. [[CrossRef](#)]
17. Batista, P.V.G.; Davies, J.; Silva, M.L.N.; Quinton, J.N. On the evaluation of soil erosion models: Are we doing enough? *Earth Sci. Rev.* **2019**, *197*, 102898. [[CrossRef](#)]
18. McGehee, R.P.; Flanagan, D.C.; Srivastava, P.; Engel, B.A.; Huang, C.-H.; Nearing, M.A. An updated isoerodent map of the conterminous United States. *Int. Soil Water Conserv. Res.* **2022**, *10*, 1–16. [[CrossRef](#)]
19. Kinnell, P.I.A.; Risse, L.M. USLE-M: Empirical Modeling Rainfall Erosion through Runoff and Sediment Concentration. *Soil Sci. Soc. Am. J.* **1998**, *62*, 1667–1672. [[CrossRef](#)]
20. Kinnell, P. Event soil loss, runoff and the Universal Soil Loss Equation family of models: A review. *J. Hydrol.* **2010**, *385*, 384–397. [[CrossRef](#)]
21. Bagarello, V.; Di Piazza, G.V.; Ferro, V.; Giordano, G. Predicting unit plot soil loss in Sicily, south Italy. *Hydrol. Process.* **2008**, *22*, 586–595. [[CrossRef](#)]
22. Bagarello, V.; Ferro, V.; Pampalone, V. A new version of the USLE-MM for predicting bare plot soil loss at the Sparacia (South Italy) experimental site. *Hydrol. Process.* **2015**, *29*, 4210–4219. [[CrossRef](#)]
23. Bagarello, V.; Di Stefano, C.; Ferro, V.; Pampalone, V. Comparing theoretically supported rainfall-runoff erosivity factors at the Sparacia (South Italy) experimental site. *Hydrol. Process.* **2018**, *32*, 507–515. [[CrossRef](#)]
24. Di Stefano, C.; Pampalone, V.; Todisco, F.; Vergni, L.; Ferro, V. Testing the Universal Soil Loss Equation-MB equation in plots in Central and South Italy. *Hydrol. Process.* **2019**, *33*, 2422–2433. [[CrossRef](#)]
25. Bagarello, V.; Ferro, V.; Flanagan, D. Predicting plot soil loss by empirical and process-oriented approaches. A review. *J. Agric. Eng.* **2018**, *49*, 1–18. [[CrossRef](#)]
26. Di Stefano, C.; Palmeri, V.; Pampalone, V. An automatic approach for rill network extraction to measure rill erosion by ter-restrial and low-cost UAV photogrammetry. *Hydrol. Process.* **2019**, *33*, 1883–1895.
27. Pampalone, V.; Carollo, F.G.; Nicosia, A.; Palmeri, V.; Di Stefano, C.; Bagarello, V.; Ferro, V. Measurement of Water Soil Erosion at Sparacia Experimental Area (Southern Italy): A Summary of More than Twenty Years of Scientific Activity. *Water* **2022**, *14*, 1881. [[CrossRef](#)]
28. Wischmeier, W.H.; Smith, D.D. *Predicting Rainfall-Erosion Losses—A Guide to Conservation Farming*; USDA Agricultural Handbook no. 537; USDA: Blacksburg, VA, USA, 1978.
29. Di Stefano, C.; Ferro, V.; Pampalone, V. Applying the USLE Family of Models at the Sparacia (South Italy) Experimental Site. *Land Degrad. Dev.* **2017**, *28*, 994–1004. [[CrossRef](#)]
30. Nearing, M.A. A Single, Continuous Function for Slope Steepness Influence on Soil Loss. *Soil Sci. Soc. Am. J.* **1997**, *61*, 917–919. [[CrossRef](#)]
31. Zhang, G.-H.; Liu, Y.-M.; Han, Y.-F.; Zhang, X.C. Sediment Transport and Soil Detachment on Steep Slopes: I. Transport Capacity Estimation. *Soil Sci. Soc. Am. J.* **2009**, *73*, 1291–1297. [[CrossRef](#)]
32. Bagarello, V.; Di Stefano, C.; Ferro, V.; Giordano, G.; Iovino, M.; Pampalone, V. Estimating the USLE Soil Erodibility Factor in Sicily, South Italy. *Appl. Eng. Agric.* **2012**, *28*, 199–206. [[CrossRef](#)]
33. Mutchler, C.K.; Carter, C.E. Soil Erodibility Variation During the Year. *Trans. ASAE* **1983**, *26*, 1102–1104. [[CrossRef](#)]
34. Torri, D.; Borselli, L.; Guzzetti, F.; Calzolari, C.; Bazzoffi, P.; Ungaro, F.; Salvador Sanchis, M.P. Soil erosion in Italy: An overview. In *Soil Erosion in Europe*; Boardman, J., Poesen, J., Eds.; Wiley: New York, NY, USA, 2006; pp. 245–261.
35. Zanchi, C. Soil loss and seasonal variation of erodibility in two soils with different texture in the Mugello valley in Central Italy. *Catena Suppl.* **1988**, *12*, 167–174.

36. Boix-Fayos, C.; Calvo-Cases, A.; Imeson, A.C.; Soriano-Soto, M.D.; Tiemessen, I.R. Spatial and short-term temporal variations in runoff, soil aggregation and other soil properties along a Mediterranean climatological gradient. *Catena* **1998**, *33*, 123–138. [[CrossRef](#)]
37. Boix-Fayos, C.; Calvo-Cases, A.; Imeson, A.C.; Soriano-Soto, M.D. Influence of soil properties on the aggregation of some Mediterranean soils and use of aggregate size and stability as land degradation indicators. *Catena* **2001**, *44*, 47–67. [[CrossRef](#)]
38. Al-Durrah, M.; Bradford, J.M. New Methods of Studying Soil Detachment due to Waterdrop Impact. *Soil Sci. Soc. Am. J.* **1981**, *45*, 949–953. [[CrossRef](#)]
39. Hussein, M.H.; Kariem, T.H.; Othman, A.K. Predicting soil erodibility in northern Iraq using natural runoff plot data. *Soil Tillage Res.* **2007**, *94*, 220–228. [[CrossRef](#)]
40. Bagarello, V.; Ferro, V. Scale Effects on Plot Runoff and Soil Erosion in a Mediterranean Environment. *Vadose Zone J.* **2017**, *16*, 1–14. [[CrossRef](#)]
41. Bagarello, V.; Ferro, V.; Pampalone, V. Testing assumptions and procedures to empirically predict bare plot soil loss in a Mediterranean environment. *Hydrol. Process.* **2015**, *29*, 2414–2424. [[CrossRef](#)]
42. Bagarello, V.; Ferro, V. Analysis of soil loss data from plots of differing length for the Sparacia experimental area, Sicily, Italy. *Biosyst. Eng.* **2010**, *105*, 411–422. [[CrossRef](#)]
43. Bagarello, V.; Ferro, V.; Giordano, G.; Mannocchi, F.; Pampalone, V.; Todisco, F.; Vergni, L. Effect of plot size on measured soil loss for two Italian experimental sites. *Biosyst. Eng.* **2011**, *108*, 18–27. [[CrossRef](#)]
44. Gao, G.Y.; Fu, B.J.; Lü, Y.H.; Liu, Y.; Wang, S.; Zhou, J. Coupling the modified SCS-CN and RUSLE models to simulate hydro-logical effects of restoring vegetation in the Loess Plateau of China. *Hydrol. Earth Syst. Sci. Discuss.* **2012**, *16*, 2347–2364. [[CrossRef](#)]
45. Shi, W.; Huang, M.; Barbour, S.L. Storm-based CSLE that incorporates the estimated runoff for soil loss prediction on the Chinese Loess Plateau. *Soil Tillage Res.* **2018**, *180*, 137–147. [[CrossRef](#)]
46. Todisco, F.; Brocca, L.; Mannocchi, F.; Melone, F.; Moramarco, T. Utilizzo di modellistica idrologica in continuo accoppiata ad un modello USLE modificato per la previsione della perdita di suolo parcellare in Umbria. *Quad. Idronomia Mont.* **2012**, *30*, 353–362, (In Italian with English Abstract).
47. Todisco, F.; Vergni, L.; Vinci, A.; Pampalone, V. Practical thresholds to distinguish erosive and rill rainfall events. *J. Hydrol.* **2019**, *579*, 124173. [[CrossRef](#)]

Disclaimer/Publisher’s Note: The statements, opinions and data contained in all publications are solely those of the individual author(s) and contributor(s) and not of MDPI and/or the editor(s). MDPI and/or the editor(s) disclaim responsibility for any injury to people or property resulting from any ideas, methods, instructions or products referred to in the content.